Direct detections of dark matter in the presence of non-standard neutrino interactions

Wei Chao, Jian-Guo Jiang, Xuan Wang and Xing-Yu Zhang

Center for Advanced Quantum Studies, Department of Physics, Beijing Normal University,
No. 19 Xin jie kou wai street, Beijing, 100875, China

E-mail: chaowei@bnu.edu.cn, jgjiang@mail.bnu.edu.cn,
xuanwang@mail.bnu.edu.cn, zhangxingyu@mail.bnu.edu.cn

Abstract. In this paper we investigate impacts of non-standard neutrino interactions (NSIs) to the limitations on the discovery potential of dark matter in direct detection experiments. New neutrino floors are derived taking into account current upper bounds on the effective couplings of various NSIs. Our study shows that the neutrino floors of the standard model neutral current interactions can be significantly changed in the presence of vector-current NSI and scalar-current NSI, and the neutrino floors can be raised up to about $\mathcal{O}(20\%)$ in the presence of pseudo-scalar-current NSI, and there are almost no impacts to the neutrino floors from the axial-vector NSI and the tensor NSI. We suggest combining the dark matter direct detection experiments with the coherent elastic neutrino nucleus scattering experiments to hunt for new physics behind the signal of nuclear recoil in the future.

JCAP08(2019)010

https://doi.org/10.1088/1475-7516/2019/08/010

Contents

1 Introduction

Cosmological observations have confirmed the existence of dark matter (DM), which points to the new physics beyond the standard model (SM). Weakly interacting massive particles (WIMP) have been taken as the most attractive DM candidate, as it can naturally address the observed relic abundance with a weak coupling to the SM particles and an electroweak scale mass. DM direct detection experiments attempt to detect the recoil energy of nuclei coming from the collisions of nuclei with WIMP in underground laboratories. For the past decades, the detection sensitivity and efficiency of DM direct detection experiments have been greatly improved, but still no signal was observed, which on the other hand puts exclusion limits on the WIMP-nucleus scattering cross section. It is well-known that the exclusion limits will soon reach the "neutrino floor" [1–3], the background from coherent elastic scattering of neutrinos off nuclei. It will be impossible to distinguish the signal of WIMP from that of neutrino using current direct detection techniques when the signal lies below the neutrino floor.

Several attempts have been made to discriminate the DM signal under the neutrino floor, which include combing data from different targets for WIMP with spin-dependent interactions [4], looking for annual modulation [5, 6], and (or) measuring the recoil momentum [7, 8]. It has been shown in ref. [9] that it is possible to lift the signal degeneracy associated with the neutrino floor for inelastic scattering. Actually, we need to understand the neutrino interactions pretty well before making further comparison. Exotic new physics may affect the neutrino floor. It has been shown in ref. [10] that the neutrino floor can be lifted by several orders of magnitude for DM mass below $10\,\mathrm{GeV}$ in the light scalar mediator case, and a factor of two in light vector mediator case. In refs. [11–14], authors have studied the effect of non-standard neutrino interactions (NSI) in the DM direct detection experiments. NSI can enhance or deplete the neutrino-nucleus event rate and thus the neutrino floor can be lifted or submerged.

In this paper we revisit impacts of NSIs to the limitations on the discovery potential of dark matter in direct detection experiments. Recently coherent elastic neutrino-nucleus scattering (CEνNS), predicted by the SM, was observed by the COHERENT experiment [15]. CEνNS allows us to study constraints on effective couplings of NSIs. After having considered

all updated upper limits, we evaluated the new neutrino floor induced by the NSIs. Our results show that the neutrino floors of the standard model neutral current interactions can be significantly changed in the presence of vector-current NSI and scalar-current NSI, and the neutrino floors can be raised up to about $\mathcal{O}(20\%)$ in the presence of pseudo-scalar-current NSI, and there are almost no impacts to the neutrino floors from the axial-vector NSI and the tensor NSI. That is to say, a signal above our new neutrino floors will be definitely that of DM, while the new physics behind a signal lying between the new and the SM neutrino floors will be blurred and indistinct, in which case one needs combine DM direct detections experiments with CEνNS experiments to make further identification. For a signal lying below the SM neutrino floors, we need to develop new direct detection methods.

The remaining of the paper is organized as follows: in section 2 we present the exotic neutrino interactions and cross section of CEνNS process. Section 3 is focused on constraints on the effective couplings of NSIs. In section 4 we present impacts of these new interactions to the neutrino floor. The last part is concluding remarks. Nuclear response function are listed in the appendix A.

2 Non-standard neutrino interactions

In the SM, CEνNS is mediated by the Z-boson at the tree level. The solar, atmosphere, accelerator and reactor neutrino oscillation experiments have confirmed that neutrinos are massive and lepton flavors are mixed, which point to new physics beyond the SM. As a result, neutrinos could interact with SM particles in the presence of new mediators (new gauge bosons or new scalar fields). Effective operators induced by these new mediators are called NSI, which is first addressed by L. Wolfenstein in the consideration of neutrino oscillation in matter [16]. In this section we address all exotic neutrino interactions beyond the original NSI which is vector-current interactions between neutrinos and quarks. It is well-known that there are 16 independent Dirac field bilinears, which can be decomposed into scalar, vector, pseudo-scalar, axial-vector and tensor currents. The most general dimension-6 operators describing effective neutrino-quark interactions can thus be written as

$$\frac{G_F}{\sqrt{2}} \sum_i \bar{\nu}_\alpha \Gamma^i P_L \nu_\beta \bar{q}_f \Gamma_i \zeta_i q_f \tag{2.1}$$

where G_F is the Fermi constant, α, β are flavors of neutrinos, $f(\equiv u, d, s)$ are flavors of quarks, ζ_i are dimensionless couplings, and

$$\Gamma_i = \left\{ 1, \, \gamma^5, \, \gamma^\mu, \, \gamma^\mu \gamma^5, \, \sigma^{\mu\nu} \right\} . \tag{2.2}$$

The Lagrangian given in eq. (2.1) may come from integrating out new or SM neutral bosons in effective field theory approach. It would be more accurate if one performs calculation in an ultraviolet (UV) completion model. However effective operator is good enough in investigating low energy neutrino-nucleus scattering and provides a model independent prediction. It should be mentioned that there are higher dimensional (dimension 7 or 8) effective operators [17], whose constraints as well as effects in DM direct detections will be presented in a future project. The Wilson coefficients relevant to the standard effective neutrino-quark interactions can be derived by integrating out Z boson

$$\zeta_{V, \, u(d,s)} = \mp \left(1 - \frac{8(4)}{3} s_W^2 \right) \delta_{\alpha\beta} , \qquad \zeta_{A, \, u(d,s)} = \pm \delta_{\alpha\beta} \tag{2.3}$$

where $s_W^2 = \sin^2 \theta_W \approx 0.238$, with θ_W the weak mixing angle.

Quark level	Nucleon level	Matching conditions
$\frac{G_F}{\sqrt{2}}\zeta_{q,S}\bar{\nu}_\alpha P_L \nu_\beta \bar{q}q$	$\frac{G_F}{\sqrt{2}}\zeta_{N,S}\bar{\nu}_\alpha P_L \nu_\beta \bar{N}N$	$\zeta_{N,S} = \sum_{q=u,d}\zeta_{q,S}\frac{m_N}{m_q}f_{T_q}^N$
$\frac{G_F}{\sqrt{2}}\zeta_{q,P}\bar{\nu}_\alpha P_L \nu_\beta \bar{q}i\gamma^5 q$	$\frac{G_F}{\sqrt{2}}\zeta_{N,P}\bar{\nu}_\alpha P_L \nu_\beta \bar{N}i\gamma^5 N$	$\zeta_{N,P} = \sum_{q=u,d}\zeta_{q,P}\frac{m_N}{m_q}\left(1-\frac{\bar{m}}{m_q}\right)\Delta_q^N$
$\frac{G_F}{\sqrt{2}}\zeta_{q,V}\bar{\nu}_\alpha \gamma_\mu P_L \nu_\beta \bar{q}\gamma^\mu q$	$\frac{G_F}{\sqrt{2}}\zeta_{N,V}\bar{\nu}_\alpha \gamma_\mu P_L \nu_\beta \bar{N}\gamma^\mu N$	$\zeta_{p,V} = 2\zeta_{u,V}+\zeta_{d,V}; \quad \zeta_{n,V} = \zeta_{u,V}+2\zeta_{d,V}$
$\frac{G_F}{\sqrt{2}}\zeta_{q,A}\bar{\nu}_\alpha \gamma_\mu P_L \nu_\beta \bar{q}\gamma^\mu\gamma^5 q$	$\frac{G_F}{\sqrt{2}}\zeta_{N,A}\bar{\nu}_\alpha \gamma_\mu P_L \nu_\beta \bar{N}\gamma^\mu\gamma^5 N$	$\zeta_{N,A} = \sum_q \zeta_{q,A}\Delta_q^N$
$\frac{G_F}{\sqrt{2}}\zeta_{q,T}\bar{\nu}_\alpha \sigma_{\mu\nu} P_L \nu_\beta \bar{q}\sigma^{\mu\nu} q$	$\frac{G_F}{\sqrt{2}}\zeta_{N,T}\bar{\nu}_\alpha \sigma_{\mu\nu} P_L \nu_\beta \bar{N}\sigma^{\mu\nu} N$	$\zeta_{N,T} = \sum_q \zeta_{q,T}\delta_q^N$

Table 1. Effective operators from the quark level to the nucleon level and the nucleon form factors.

To calculate the cross section of CEνNS, one needs to match the effective operators given in eq. (2.1) onto effective field theory describing interactions between neutrinos and non-relativistic nucleon, which was done in refs. [18, 19]. We list in the table. 1 the relevant form factors, in which we have ignored the q^2 dependence. $f_{T_q}^N \equiv (\langle N|m_q\bar{q}q|N\rangle/m_N)$ express the light quark contribution to the nucleon mass, $\bar{m} = (1/m_u+1/m_d+1/m_s)^{-1}$, Δ_q^N parameterize the quark spin content of the nucleon, δ_q^N are the difference between the spin of quarks and that of anti-quarks in nucleon, m_N is the mass of nucleon.

Before preceding to the calculation of CEνNS cross section, one needs to evaluate effective couplings between neutrinos and the proton or the neutron. We assume neutrinos couple to u-quark and d-quark universally in NSI, i.e. $\zeta_{u,i} = \zeta_{d,i} = \zeta_i$, since the neutral currents are usually blinded to the isospin. As a result, $\zeta_{p,V} = \zeta_{n,V} = 3\zeta_V$, $\zeta_{p,A} = \zeta_{n,A} = 0.41\zeta_A$ since $\Delta_u^p = \Delta_d^n = 0.84$ and $\Delta_d^p = \Delta_u^n = -0.43$ [20], $\zeta_{p,T} = \zeta_{n,T} = 0.61\zeta_T$ as $\delta_u^p = \delta_d^n = 0.84$ and $\delta_d^p = \delta_u^n = -0.23$ [21], $\zeta_{p,S} \approx \zeta_{n,S} = 16.3\zeta_S$ by using inputs of $f_{T_q}^{p,n}$ provided in ref. [20], $\zeta_{p,P} \approx 59\zeta_P$ and $\zeta_{n,P} \approx 55\zeta_P$.

The differential cross section of CEνNS in the present of NSIs is calculated in refs. [22, 23]. For our case, it can be written as

$$
\frac{d\sigma_\nu}{dE_R} = \frac{2G_F^2 m_A}{(2J_A+1)E_\nu^2}\Bigg\{ \sum_{\alpha\beta=0,1}(4E_\nu^2-2m_A E_R)\zeta_V^\alpha \zeta_V^{\beta*}W_M^{\alpha\beta}(q^2)
$$
$$
+ \sum_{\alpha,\beta=0,1}\left(E_\nu^2+\frac{1}{2}m_A E_R\right)\zeta_A^\alpha \zeta_A^{\beta*}W_{\Sigma'}^{\alpha\beta}(q^2) + \sum_{\alpha\beta=0,1}\frac{E_R}{4m_A}(2E_\nu^2-m_A E_R)\zeta_A^\alpha \zeta_A^{\beta*}W_{\Sigma''}^{\alpha\beta}(q^2)
$$
$$
+ 8(2E_\nu^2-m_A E_R)\zeta_T^2 W_{\Sigma'}^{00}(q^2) + 16E_\nu^2\zeta_T^2 W_{\Sigma''}^{00}(q^2) + 2m_A E_R\zeta_S^2 W_M^{00}(q^2)
$$
$$
+ \sum_{\alpha\beta=0,1}\frac{E_R^2 m_A^2}{m_N^2}\zeta_P^\alpha \zeta_P^{\beta*}W_{\Sigma''}^{\alpha\beta}(q^2)\Bigg\} \tag{2.4}
$$

where $W_{M,\Sigma',\Sigma''}^{\alpha\beta}(q^2)$ are the nuclear response functions, E_ν is the initial neutrino energy, E_R is the recoil energy of the nucleus, J_A is the spin of target nuclei, $\zeta_X^0 = \frac{1}{2}(\zeta_{p,X}+\zeta_{n,X})$ and $\zeta_X^1 = \frac{1}{2}(\zeta_{p,X}-\zeta_{n,X})$, m_A is the mass of target nuclei. Numerical expressions of $W_{M,\Sigma',\Sigma''}^{\alpha\beta}(q^2)$ are given in the appendix A, which are taken from the public code "**dmformfactor**" in ref. [25].

3 Constraints

Before proceeding to the study of neutrino floor, we summarize in this section constraints on the NSI Wilson coefficients, arising from neutrino oscillations, CEνNS and deep inelastic

Couplings	Constraints	Couplings	Constraints	Couplings	Constraints	Couplings	Constraints
$\zeta^{eX}_{u,S}$	0.051	$\zeta^{\mu X}_{u,S}$	0.035	$\zeta^{eX}_{u,P}$	4.863	$\zeta^{\mu X}_{u,P}$	0.484
$\zeta^{eX}_{d,S}$	0.051	$\zeta^{\mu X}_{d,S}$	0.034	$\zeta^{eX}_{d,P}$	6.256	$\zeta^{\mu X}_{d,P}$	0.686
$\zeta^{eX}_{s,S}$	0.866	$\zeta^{\mu X}_{s,S}$	0.579	$\zeta^{eX}_{s,P}$	11.87	$\zeta^{\mu X}_{s,P}$	1.603
$\zeta^{eX}_{u,T}$	0.632	$\zeta^{\mu X}_{u,T}$	0.064	$\zeta^{eX}_{u,A}$	0.996	$\zeta^{\mu X}_{u,A}$	0.178
$\zeta^{eX}_{d,T}$	0.866	$\zeta^{\mu X}_{d,T}$	0.093	$\zeta^{eX}_{d,A}$	0.996	$\zeta^{\mu X}_{d,A}$	0.250
$\zeta^{eX}_{s,T}$	1.680	$\zeta^{\mu X}_{s,T}$	0.215	$\zeta^{eX}_{s,A}$	2.123	$\zeta^{\mu X}_{s,A}$	0.500
$\zeta^{eX}_{u,V}$	0.123	$\zeta^{\mu X}_{u,V}$	0.084				
$\zeta^{eX}_{d,V}$	0.112	$\zeta^{\mu X}_{d,V}$	0.072				
$\zeta^{eX}_{s,V}$	2.123	$\zeta^{\mu X}_{s,V}$	0.566				

Table 2. Upper limits on the effective couplings.

scattering (DIS). According to global fits to oscillation data, one has [23, 36]

$$\zeta^{ee}_{u,V} \in (-0.080,\ 0.618)\,, \qquad \zeta^{ee}_{d,V} \in (-0.012,\ 0.361)\,,$$
$$\zeta^{\mu\mu}_{u,V} \in (-0.111,\ 0.402)\,, \qquad \zeta^{\mu\mu}_{d,V} \in (-0.103,\ 0.361)\,, \qquad (3.1)$$

at the 95% C.L.. Constraints of CEνNS and DIS are separately given by the COHER-ENT [15, 26] and CHARM [27] collaborations. Since these constraints were already studied in references, we will not repeat the investigation here. We list in the table. 2 the most stringent current or predicted constraints on $\zeta_{q,X}$, which are derived by translating results of table. II and III in ref. [23] into the upper bounds of $\zeta_{q,X}$ in our case. Collider constraints on couplings of NSI [24] will not be considered in our analysis.

4 Neutrino floor

DM direct detection experiments, which are designed to search for the nuclear recoil in the scattering of WIMPs off nuclei, probe DM straightforwardly. There are many on the running or designed DM direct detection experiments on the world, for a review of direct detection experiments and their current status, see [28, 29] and references therein for detail. The WIMP event rate can be written as [30]

$$\frac{dR}{dE_R} = MT \times \frac{\rho_{\rm DM}\sigma^0_n A^2}{2m_{\rm DM}\mu^2_n} F^2(E_R) \int_{v_{\rm min}} \frac{f(\vec{v})}{v} d^3v \qquad (4.1)$$

where M is the target mass, T is the exposure time, $\rho_{\rm DM} = 0.3$ GeV/c^2/cm^3 being the DM density in the local halo, μ_n is the nucleon-DM reduced mass, σ^0_n is the DM-nucleon cross section, A is the atomic number, $F(E_R)$ is the nuclear form factor and we use the Helm form factor [31], $f(\vec{v})$ is assumed to be the Maxwell-Boltzmann distribution function describing the DM velocity distribution in the Earth frame, $v_{\rm min}$ depends on E_R: $v_{\rm min} = \sqrt{m_N E_R/2\mu^2_N}$ with μ_N the DM-nucleus reduced mass. The velocity integral in eq. (4.1) can be analytically written as [32]

$$\int_{v_{\rm min}} \frac{f(\vec{v})}{v} d^3v = \frac{1}{2v_0\eta_E} \left[{\rm erf}(\eta_+) - {\rm erf}(\eta_-) \right] - \frac{1}{\pi v_0\eta_E}(\eta_+ - \eta_-)e^{-\eta^2_{\rm esc}} \qquad (4.2)$$

where v_0 is the speed of the Local Standard of Rest, $\eta_E = v_E/v_0$ with v_E the Earth velocity with respect to the galactic center, $\eta_{\rm esc} = v_{\rm esc}/v_0$ with $v_{\rm esc}$ the escape velocity of DM from

our galaxy, $\eta_\pm = \min(v_{\min}/v_0 \pm \eta_E, v_{\rm esc}/v_0)$. We take $v_0 = 220$ km/s, $v_{\rm esc} = 544$ km/s and $\vec{v}_E = \vec{v}_\odot + \vec{v}_\oplus \approx \vec{v}_\odot = 232$ km/s, where $\vec{v}_\odot$ and $\vec{v}_\oplus$ are the velocity of the sun with respect to the Galaxy as well as the Earth rotational velocity, respectively.

Although much efforts are made to improve the detection sensitivity and efficiency, no DM signal was observed in any direct detection experiments. The 90% CL upper bound on the zero observed counts is 2.3 event [33], so we can get the exclusion limit on the direct detection cross section in the $m_{\rm DM} - \sigma_n^0$ plane for a concrete direct detection experiment with fixed exposure, by requiring $\int dR/dE_R \varepsilon(E_R) dE_R < 2.3$, where $\varepsilon(E_R)$ is the detector efficiency function and is set to be 1 in our following analysis.

It is well-known that the exclusion of the spin-independent direct detection cross section will soon reach the neutrino floor, below which the spectrum of the recoil energy induced by WIMP-nucleus scattering can not be distinguished from that induced by the CEνNS. The background is due to solar neutrinos at low recoil energies and atmosphere neutrinos or supernovae neutrinos at high recoil energies. Some approaches were proposed on how to extract DM signature from below the neutrino floors. Here we focus on the neutrino floor itself and evaluate the impacts of exotic neutrino interactions to the neutrino floors. The event rate induced by the CEνNS can be written as

$$\frac{dR_\nu}{dE_R} = MT \times \frac{1}{m_A} \int_{E_\nu^{\min}} \frac{d\phi_\nu}{dE_\nu} \frac{d\sigma_\nu}{dE_R} dE_\nu \tag{4.3}$$

where $d\phi_\nu/dE_\nu$ is the flux of neutrinos, $d\sigma_\nu/dE_R$ is the differential cross section of CEνNS given in eq. (2.4). The relevant flux used in our analysis are taken from refs. [34, 35]. The minimum energy of neutrinos, $E_\nu^{\min}$, required to induce a nuclear recoil at the energy E_R is $\sqrt{m_A E_R/2}$.

For a given target, one can construct the neutrino floor in the following way: first, calculating the exposure required to generate n counts of CEνNS for a given minimum energy threshold. Second, computing the spin-independent WIMP-nucleon cross section using the following master equation,

$$\sigma_n^0 = \frac{2.3}{n} \int_{E_R} \left(\frac{1}{m_N} \int_{E_\nu^{\min}} \frac{d\phi_\nu}{dE_\nu} \frac{d\sigma_\nu}{dE_R} \right) \left(\frac{\rho_{\rm DM} A^2}{2 m_{\rm DM} \mu_n^2} \int_{E_R}^{E_R^{\max}} F^2(E_R) dE_R \int_{v_{\min}} \frac{f(\vec{v})}{v} d^3 v \right)^{-1}. \tag{4.4}$$

With this equation, one can get the neutrino floor with n neutrino events and estimate the impactions of NSIs to the direct detections of DM.

5 Results

Taking into account the upper bound on the effective couplings of NSI, the cross section of CEνNS can be significantly changed. We first evaluate impacts of NSIs to the neutrino event rate. In the first row of the figure 1, we show the event rate as the function of the recoil energy in the Xe131 target in the presence of a single NSI, where plots in the left-panel and right-panel correspond to the vector-current NSI and the scalar-current NSI respectively. The red solid lines in both plots are the cases of SM neutrino interaction, while the blue dashed lines are cases with additional NSI. Notice that the shape of the curve with additional vector-current NSI is similar to that of the SM case, while the behavior of the curve with additional scalar-current NSI is very different from the SM one. This is because the vector-current NSI interferes with the SM contribution and only change the size of the effective coupling, while
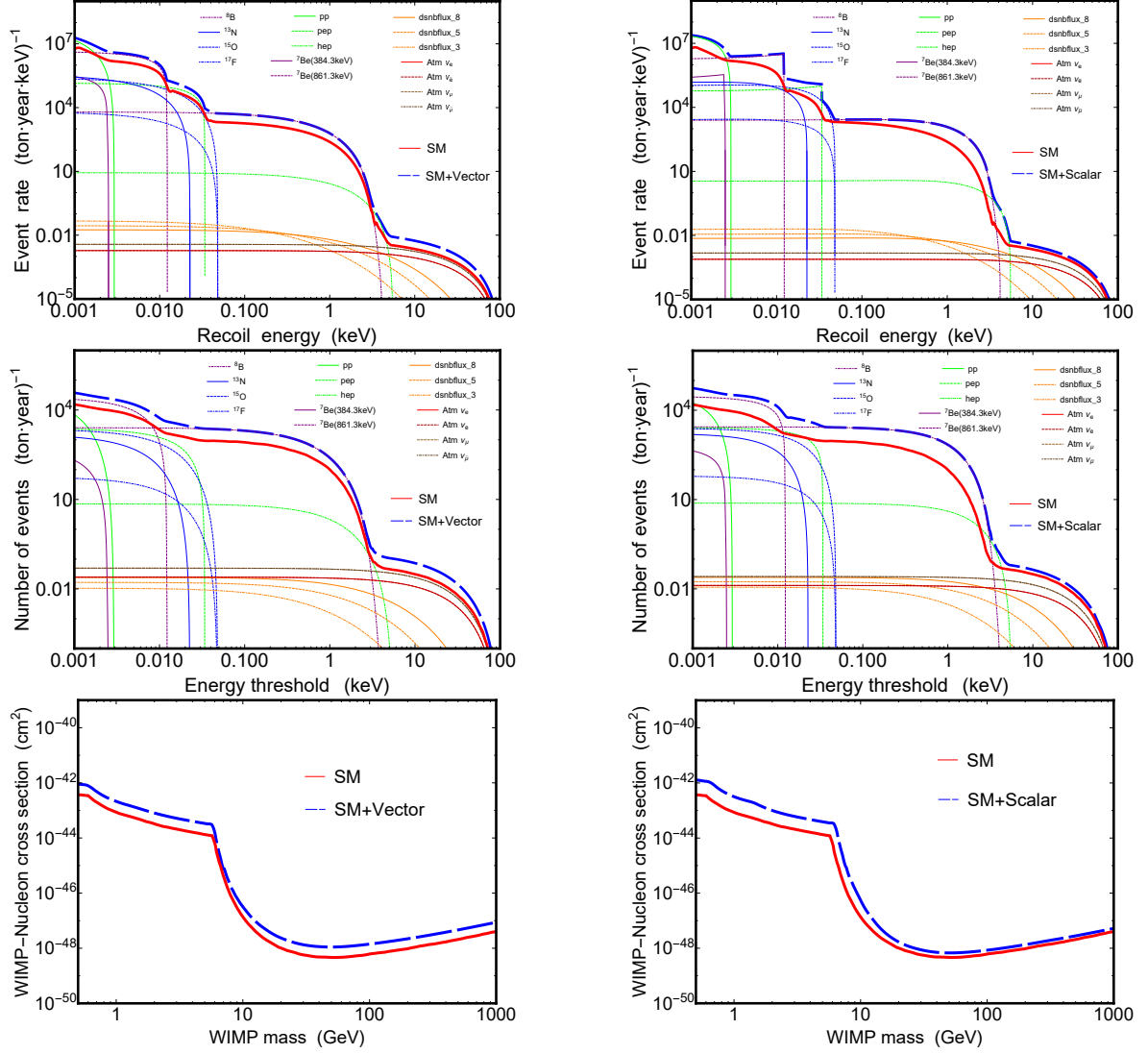
Figure 1. First row: event rate as the function of the recoil energy in the Xe131 target in the presence of a single vector current NSI (left-panel) and single scalar current NSI (right-panel). Second row: number of event as the function of energy threshold in the presence of a single vector current NSI (left-panel) and single scalar current NSI (right-panel). Third row: neutrino floor as the function of dark matter mass in the presence of a single vector current NSI (left-panel) and single scalar current NSI (right-panel).

the scattering cross section from the scalar-current NSI is only coherently enhanced and there is no interference with the SM contribution. In addition, dependences of the cross section on the recoil energy in scalar-current and vector-current are different, as can be seen from the eq. (2.4).

We show in the second row of the figure 1 number of CEνNS events generated within one ton·year exposure in the Xe131 target as the function of energy threshold for vector-current NSI (left-panel) and scalar-current NSI (right-panel) respectively. We have set an upper bound (100 keV) on the nuclear recoil energy when making the plot. Plots may be changed according to this upper limit. Number of events can be significantly enhanced for both low
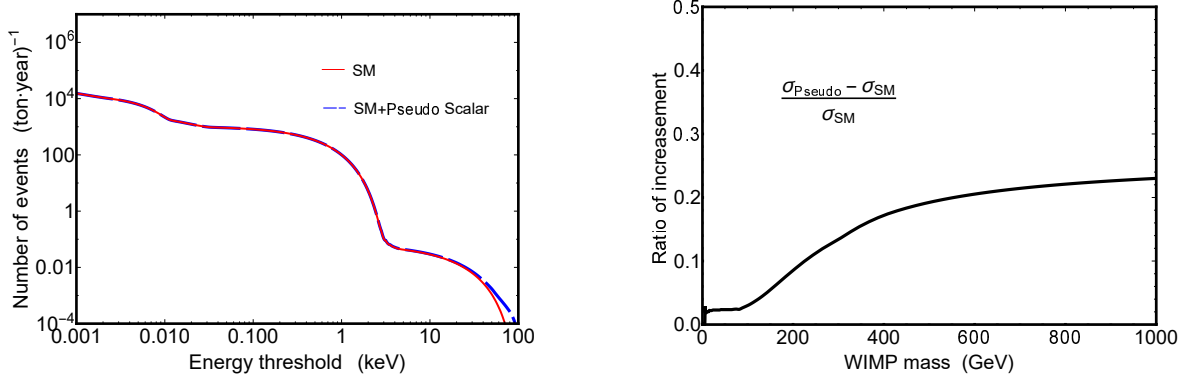
Figure 2. Left-panel: neutrino events as the function of the energy threshold in the Xe-131 detector in the presence of a single pseudo-scalar current NSI; right-panel: enhancement of the neutrino floor with respect to the SM case.

and high energy threshold in the presence of vector-current NSI, and number of events is only enhanced for low energy threshold in presence of scalar-current NSI. It is because there is no interference between the SM contribution and that from the scalar-current NSI [37], thus the relative enhancement will significantly decrease with the increase of the threshold energy.

We show in the third row of the figure 1 the neutrino floor in the Xe131 target as the function of dark matter mass for vector-current (left-panel) NSI and scalar-current (right-panel) NSI respectively. The red solid lines are the SM case and the blue dashed lines are cases with additional NSIs. Each point in curves corresponds to the WIMP-nucleon scattering cross section in the exposure where one CEνNS event is generated that can not be distinguished from the WIMP event. To make the plot, we first evaluate the exposure such that Xe131 target expects one neutrino event, with varying energy threshold from 10^{-3} keV to 100 keV. Then we calculate the WIMP-nucleon scattering cross section for each exposure by requiring $\int dR/dE_R \varepsilon(E_R) = 2.3$. By taking the smallest cross section for various energy threshold at a fixed dark matter mass, that corresponds to the best background free sensitivity estimate achievable, one can draw the curve. As can be seen, neutrino floors can be significantly raised by the vector-current NSI in both low and high dark matter mass region, and the neutrino floors can be raised by scalar-current NSI only in low dark matter mass region.

We show in the left-panel of the figure 2 number of neutrino event within 1 ton·year exposure in the Xe131 target as the function of energy threshold for pseudo-scalar-current NSI (blue dashed line). As can be seen, the enhancement is tiny for small energy threshold, this is because the contribution of the pseudo-scalar current NSI to the CEνNS is suppressed by the tiny nuclear response functions $W_{\Sigma''}^{\alpha\beta}(q^2)$. For a large recoil energy, its effect become significant because the contribution of the pseudo-scalar-current NSI to the CEνNS cross section is proportional to E_R^2. We show in the right-panel of the figure 2 a ratio R as the function of dark matter mass, with R defined by

$$R = \frac{\sigma_{\text{neutrino floor}}^{\text{SM+NSI}} - \sigma_{\text{neutrino floor}}^{\text{SM}}}{\sigma_{\text{neutrino floor}}^{\text{SM}}} \tag{5.1}$$

where $\sigma_{\text{neutrino floor}}^{\text{SM+NSI}}$ is the neutrino floor with pseudo-scalar-current NSI and $\sigma_{\text{neutrino floor}}^{\text{SM}}$ is the neutrino floor induced by the SM neutral current interactions. It is clear that the enhancement can be of $\mathcal{O}(20\%)$.
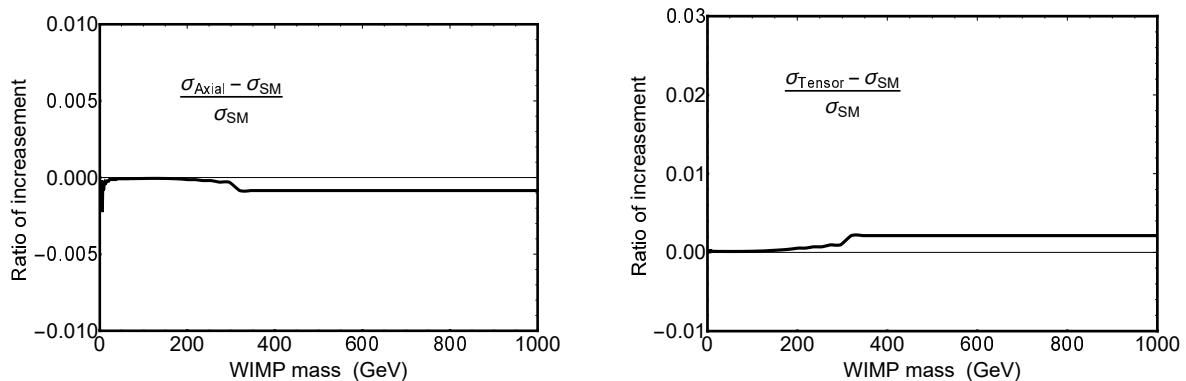
Figure 3. The ratio R as the function of dark matter mass for the axial-vector current NSI (left-panel) and tensor current NSI (right-panel).

We find that contributions of the axial-vector-current NSI and the tensor-current NSI to the CEνNS are suppressed by the nuclear response function and the enhancement to the neutrino events can be neglected. As illustrations, we show in the figure 3 the ratio R, which is defined in eq. (5.1), as the function of dark matter mass for the axial-vector-current NSI(left-panel) and tensor-current NSI (right-panel). Changes of the neutrino floor due to these two kinds of NSIs are within $\mathcal{O}(1\%)$.

For completeness, we show in the figure 4 impacts of the vector-current NSI (left-panel) and scalar current NSI (right-panel) to the neutrino floor in Ge72 target. In the first, second and third rows we show neutrino event rate as the function of recoil energy, number of CEνNS event as the function of energy threshold and the neutrino floor as the function of dark matter mass, respectively. Results are similar to these in the Xe131 case. Since the nuclear response function $W_{\Sigma',\Sigma''}^{\alpha\beta}(q^2)$ for Ge72 are null, contributions of axial-vector-current, pseudo-scalar-current and tensor-current NSIs are zero.

Notice that impacts of exotic neutrino interactions to the dark matter discovery potential of direct detection experiments have been investigated in refs. [10, 14], where they have studied effects of a vector mediator as well as a light scalar mediator in simplified models. It should be mentioned that constraints on the effective couplings arising from various process need be considered in these specific models [10, 38], and the combined constraint could be stronger than those from COHERENT and CHARM experiments. Our study differs substantially from their investigations in several respects. We take the effective field theory approach to study the neutrino floor arising from the non-standard neutrino interactions. Our conclusions are thus model independent and general, although constraints might be less stringent in certain dark matter mass range compared with specific model. And also, we have studied the effects of pseudo-scalar, axial-vector and tensor currents, which could provide guidance for further model-dependent study of the neutrino floor. In this sense, our study and theirs are largely complementary to each other.

6 Conclusion

It is well-known that there are limitations on the discovery potential of dark matter in direct detection experiments, the so-called neutrino floor. In this paper, we have examined impactions of non-standard neutrino interactions to the neutrino floor. Our results show that the neutrino floors can be significantly changed by the vector-current NSI and scalar-current
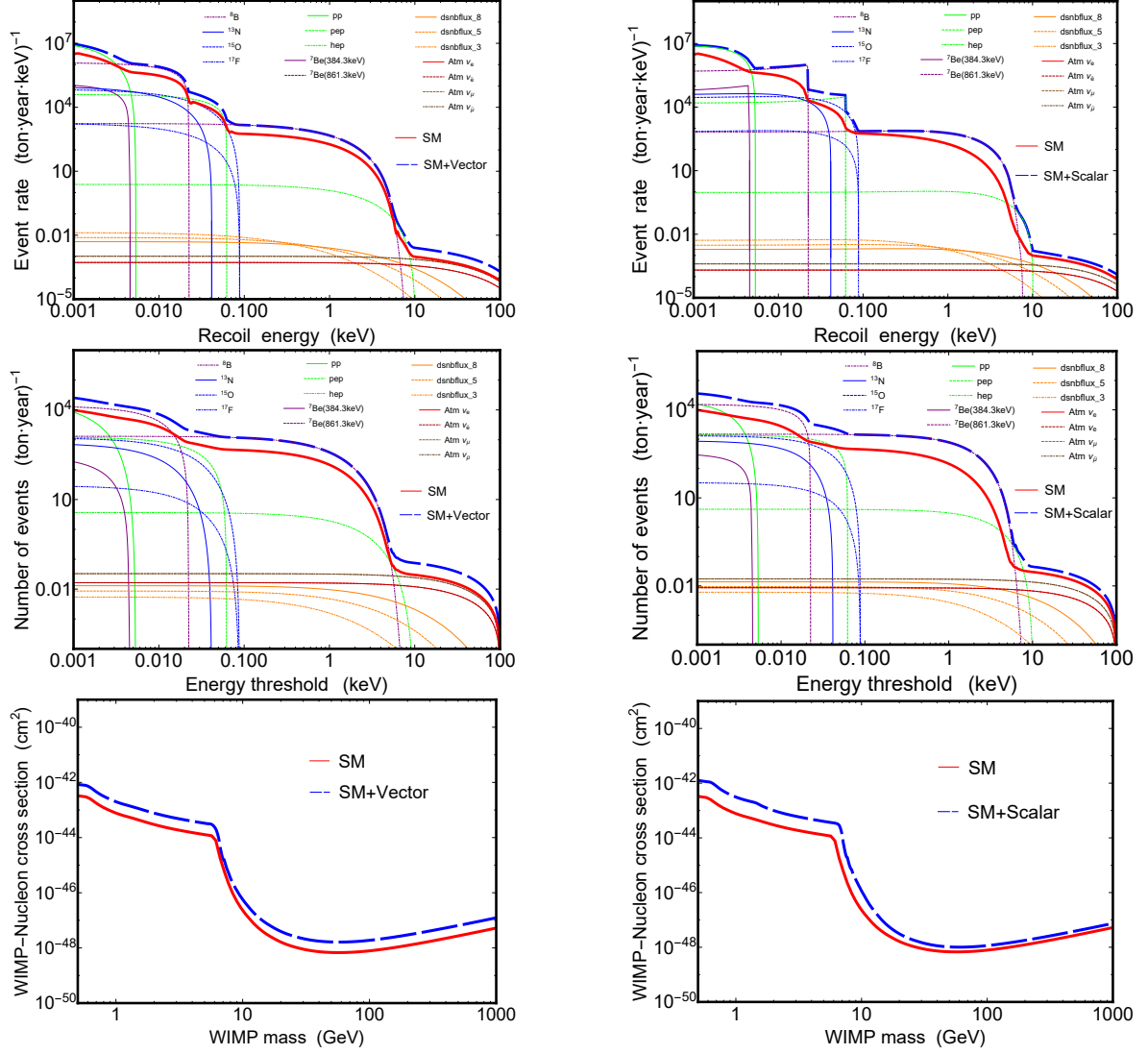
Figure 4. First row: event rate as the function of the recoil energy in the Ge72 target in the presence of a single vector current NSI (left-panel) and single scalar current NSI (right-panel). Second row: number of event as the function of energy threshold in the presence of a single vector current NSI (left-panel) and single scalar current NSI (right-panel). Third row: neutrino floor as the function of dark matter mass in the presence of a single vector current NSI (left-panel) and single scalar current NSI (right-panel).

NSI, and also it can be enhanced about $\mathcal{O}(20\%)$ by the a pseudo-scalar-current NSI, when considering the current upper bounds on couplings of NSIs. Contributions of axial-vector-current NSI and tensor-current NSI to the neutrino floor are negligible. Our study shows that one can not exactly determine whether or not it is a dark matter signal if an event is observed in the future at above the SM neutrino floors but at below our new neutrino floors. In this case, one needs to combine all constraints from neutrino experiments to discriminate the neutrino signal from the dark matter signal. No matter what it is, it will be a signal of new physics but one needs more work to reveal its nature. One will be pretty sure about the dark matter nature of the signal lying above our new neutrino floors.

Acknowledgments

A Nuclear response function

The nuclear response functions $W^{\alpha\beta}_{M,\Sigma',\Sigma''}$ of Ge72 and Xe131 are shown as following, where $y = (qb/2)^2$, $b[fm] = \sqrt{41.467/(45A^{-1/3} - 25A^{-2/3})}$ with A the isotope of interest. They are taken from the public code "**dmformfactor**" given in ref. [25].

Ge72:

$$
\begin{aligned}
W^{00}_M(y) = {}& e^{-13.9963y}(103.126 - 2092.16y + 16245.9y^2 \\
& -61392.4y^3 + 119994y^4 - 116348y^5 + 45218y^6 \\
& -1304.96y^7 + 9.79078y^8) \\
W^{01}_M(y) = {}& e^{-13.9963y}(-11.4565 + 278.503y - 2536.5y^2 + 11080.5y^3 \\
& +24762.7y^4 + 27262.6y^5 - 12055.2y^6 + +518.725y^7) \\
W^{10}_M(y) = {}& W^{01}_M(y) \\
W^{11}_M(y) = {}& e^{-13.9963y}(1.27272 - 36.0585y + 383.661y^2 - 1940.43y^3 \\
& +4984.81y^4 - 6276.89y^5 + 3186.13y^6) \\
& -182.418y^7 + 2.77608y^8 \\
W^{00}_{\Sigma'}(y) = {}& W^{01}_{\Sigma'}(y) = W^{10}_{\Sigma'}(y) = W^{11}_{\Sigma'}(y) = 0 \\
W^{00}_{\Sigma''}(y) = {}& W^{01}_{\Sigma''}(y) = W^{10}_{\Sigma''}(y) = W^{11}_{\Sigma''}(y) = 0
\end{aligned}
$$

Xe131:

$$
\begin{aligned}
W^{00}_M(y) = {}& e^{-16.6234y}(1365.52 - 45282.6y + 592353y^2 \\
& +3.97599 \times 10^6 y^3 + 1.5125 \times 10^7 y^4 - 3.38604 \times 10^7 y^5 + 4.45089 \times 10^7 y^6 \\
& -3.2834 \times 10^7 y^7 + 1.20974 \times 10^7 y^8 - 1.68685 \times 10^6 y^9 + 76997.6y^{10}) \\
W^{01}_M(y) = {}& e^{-16.6234y}(-239.705 - 9479.45y + 154341y^2 + 1.24433 \times 10^6 y^3 \\
& +5.64439 \times 10^6 y^4 + 1.4972 \times 10^7 y^5 - 2.32082 \times 10^7 y^6 + 2.01088 \times 10^7 y^7 \\
& -8.69448 \times 10^6 y^8 + 1.43961 \times 10^6 y^9 + 76997.6y^{10}) \\
W^{10}_M(y) = {}& W^{01}_M(y) \\
W^{11}_M(y) = {}& e^{-16.6234y}(42.0782 - 2027.49y + 38307.4y^2 - 368419y^3 \\
& +1.99059 \times 10^6 y^4 + 6.27412 \times 10^6 y^5 + 1.15354 \times 10^7 y^6 \\
& -1.1857 \times 10^7 y^7 + 6.08587 \times 10^6 y^8 - 1.19237 \times 10^6 y^9 + 76997.6y^{10}) \\
W^{00}_{\Sigma'}(y) = {}& e^{-16.6234y}(0.0147078 - 1.1414y + 32.683y^2 \\
& -446.814y^3 + 3401.36y^4 - 14774.3y^5 + 35758.4y^6 - 44223.9y^7 + 21252.4y^8 \\
& +962.029y^9 + 11.0398y^{10}) \\
W^{01}_{\Sigma'}(y) = {}& e^{-16.6234y}(-0.0139715 + 1.08922y - 31.6241y^2 \\
& +443.515y^3 - 3460.69y^4 + 15318.3y^5 - 37533.7y^6 + 46711.4y^7 - 22491.7y^8 \\
& -990.344y^9 - 11.0398y^{10})
\end{aligned}
$$

$$W_M^{10}(y) = W_M^{01}(y)$$

$$W_{\Sigma'}^{11}(y) = e^{-16.6234y}(0.0132721 - 1.0394y + 30.5993y^2$$
$$- 439.942y^3 + 3518.97y^4 - 15877.2y^5 + 39392.9y^6 - 49337.7y^7 + 23804.5y^8$$
$$+ 1018.66y^9 + 11.0937y^{10})$$

$$W_{\Sigma''}^{00}(y) = e^{-16.6234y}(0.00735391 + 0.199593y$$
$$- 1.3918y^2 - 21.3512y^3 + 487.152y^4 - 3498.26y^5 + 11846.8y^6 - 19238.3y^7$$
$$+ 12306.7y^8 - 116.765y^9 + 0.281202y^{10})$$

$$W_{\Sigma''}^{01}(y) = e^{-16.6234y}(-0.00698576 - 0.195462y$$
$$+ 1.27658y^2 + 21.2236y^3 - 471.84y^4 + 3383.00y^5 - 11490.7y^6 + 18739.6y^7$$
$$- 12055.6y^8 + 115.632y^9 - 0.281202y^{10})$$

$$W_{\Sigma''}^{10}(y) = W_{\Sigma''}^{01}(y)$$

$$W_{\Sigma''}^{11}(y) = e^{-16.6234y}(0.00663605 + 0.191245y$$
$$- 1.15856y^2 - 21.2101y^3 + 457.857y^4 - 3274.86y^5 + 11150.6y^6$$
$$- 18258.2y^7 + 11811.3y^8 - 114.498y^9 + 0.2812y^{10})$$

References

[1] J. Monroe and P. Fisher, *Neutrino backgrounds to dark matter searches*, *Phys. Rev.* **D 76** (2007) 033007 [arXiv:0706.3019] [INSPIRE].

[2] L.E. Strigari, *Neutrino coherent scattering rates at direct dark matter detectors*, *New J. Phys.* **11** (2009) 105011 [arXiv:0903.3630] [INSPIRE].

[3] J. Billard, L. Strigari and E. Figueroa-Feliciano, *Implication of neutrino backgrounds on the reach of next generation dark matter direct detection experiments*, *Phys. Rev.* **D 89** (2014) 023524 [arXiv:1307.5458] [INSPIRE].

[4] F. Ruppin, J. Billard, E. Figueroa-Feliciano and L. Strigari, *Complementarity of dark matter detectors in light of the neutrino background*, *Phys. Rev.* **D 90** (2014) 083510 [arXiv:1408.3581] [INSPIRE].

[5] J.H. Davis, *Dark matter vs. neutrinos: the effect of astrophysical uncertainties and timing information on the neutrino floor*, *JCAP* **03** (2015) 012 [arXiv:1412.1475] [INSPIRE].

[6] C.A.J. O'Hare, *Dark matter astrophysical uncertainties and the neutrino floor*, *Phys. Rev.* **D 94** (2016) 063527 [arXiv:1604.03858] [INSPIRE].

[7] P. Grothaus, M. Fairbairn and J. Monroe, *Directional dark matter detection beyond the neutrino bound*, *Phys. Rev.* **D 90** (2014) 055018 [arXiv:1406.5047] [INSPIRE].

[8] C.A.J. O'Hare, A.M. Green, J. Billard, E. Figueroa-Feliciano and L.E. Strigari, *Readout strategies for directional dark matter detection beyond the neutrino background*, *Phys. Rev.* **D 92** (2015) 063518 [arXiv:1505.08061] [INSPIRE].

[9] G.B. Gelmini, V. Takhistov and S.J. Witte, *Casting a wide signal net with future direct dark matter detection experiments*, *JCAP* **07** (2018) 009 [*Erratum ibid.* **02** (2019) E02] [arXiv:1804.01638] [INSPIRE].

[10] C. Bœhm, D.G. Cerdeño, P.A.N. Machado, A. Olivares-Del Campo and E. Reid, *How high is the neutrino floor?*, *JCAP* **01** (2019) 043 [arXiv:1809.06385] [INSPIRE].

[11] B. Dutta, S. Liao, L.E. Strigari and J.W. Walker, *Non-standard interactions of solar neutrinos in dark matter experiments*, *Phys. Lett.* **B 773** (2017) 242 [arXiv:1705.00661] [INSPIRE].

[12] D. Aristizabal Sierra, N. Rojas and M.H.G. Tytgat, *Neutrino non-standard interactions and dark matter searches with multi-ton scale detectors*, *JHEP* **03** (2018) 197 [arXiv:1712.09667] [INSPIRE].

[13] M.C. Gonzalez-Garcia, M. Maltoni, Y.F. Perez-Gonzalez and R. Zukanovich Funchal, *Neutrino discovery limit of dark matter direct detection experiments in the presence of non-standard interactions*, *JHEP* **07** (2018) 019 [arXiv:1803.03650] [INSPIRE].

[14] E. Bertuzzo, F.F. Deppisch, S. Kulkarni, Y.F. Perez Gonzalez and R. Zukanovich Funchal, *Dark matter and exotic neutrino interactions in direct detection searches*, *JHEP* **04** (2017) 073 [*Erratum ibid.* **04** (2017) 073] [arXiv:1701.07443] [INSPIRE].

[15] COHERENT collaboration, *Observation of coherent elastic neutrino-nucleus scattering*, *Science* **357** (2017) 1123 [arXiv:1708.01294] [INSPIRE].

[16] L. Wolfenstein, *Neutrino oscillations in matter*, *Phys. Rev.* **D 17** (1978) 2369 [INSPIRE].

[17] WORKING GROUP 3 collaboration, *Beyond the Standard Model physics at the HL-LHC and HE-LHC*, arXiv:1812.07831 [INSPIRE].

[18] A.L. Fitzpatrick, W. Haxton, E. Katz, N. Lubbers and Y. Xu, *The effective field theory of dark matter direct detection*, *JCAP* **02** (2013) 004 [arXiv:1203.3542] [INSPIRE].

[19] F. Bishara, J. Brod, B. Grinstein and J. Zupan, *From quarks to nucleons in dark matter direct detection*, *JHEP* **11** (2017) 059 [arXiv:1707.06998] [INSPIRE].

[20] P. Gondolo, J. Edsjo, P. Ullio, L. Bergstrom, M. Schelke and E.A. Baltz, *DarkSUSY: computing supersymmetric dark matter properties numerically*, *JCAP* **07** (2004) 008 [astro-ph/0406204] [INSPIRE].

[21] G. Bélanger, F. Boudjema, A. Pukhov and A. Semenov, *MicrOMEGAs$_3$: a program for calculating dark matter observables*, *Comput. Phys. Commun.* **185** (2014) 960 [arXiv:1305.0237] [INSPIRE].

[22] M. Lindner, W. Rodejohann and X.-J. Xu, *Coherent neutrino-nucleus scattering and new neutrino interactions*, *JHEP* **03** (2017) 097 [arXiv:1612.04150] [INSPIRE].

[23] W. Altmannshofer, M. Tammaro and J. Zupan, *Non-standard neutrino interactions and low energy experiments*, arXiv:1812.02778 [INSPIRE].

[24] D. Choudhury, K. Ghosh and S. Niyogi, *Probing nonstandard neutrino interactions at the LHC run II*, *Phys. Lett.* **B 784** (2018) 248 [INSPIRE].

[25] N. Anand, A.L. Fitzpatrick and W.C. Haxton, *Weakly interacting massive particle-nucleus elastic scattering response*, *Phys. Rev.* **C 89** (2014) 065501 [arXiv:1308.6288] [INSPIRE].

[26] COHERENT collaboration, *COHERENT 2018 at the spallation neutron source*, arXiv:1803.09183 [INSPIRE].

[27] X. Qian and J.-C. Peng, *Physics with reactor neutrinos*, *Rept. Prog. Phys.* **82** (2019) 036201 [arXiv:1801.05386] [INSPIRE].

[28] T. Marrodán Undagoitia and L. Rauch, *Dark matter direct-detection experiments*, *J. Phys.* **G 43** (2016) 013001 [arXiv:1509.08767] [INSPIRE].

[29] J. Liu, X. Chen and X. Ji, *Current status of direct dark matter detection experiments*, *Nature Phys.* **13** (2017) 212 [arXiv:1709.00688] [INSPIRE].

[30] J.D. Lewin and P.F. Smith, *Review of mathematics, numerical factors and corrections for dark matter experiments based on elastic nuclear recoil*, *Astropart. Phys.* **6** (1996) 87 [INSPIRE].

[31] R.H. Helm, *Inelastic and elastic scattering of 187 MeV electrons from selected even-even nuclei*, *Phys. Rev.* **104** (1956) 1466 [INSPIRE].

[32] V. Barger, W.-Y. Keung and D. Marfatia, *Electromagnetic properties of dark matter: dipole moments and charge form factor*, *Phys. Lett.* **B 696** (2011) 74 [arXiv:1007.4345] [inSPIRE].

[33] D. Goodstein, *Adventures in cosmology*, World Scientific, Hackensack, U.S.A. (2012) [inSPIRE].

[34] J.N. Bahcall and A.M. Serenelli, *How do uncertainties in the surface chemical abundances of the sun affect the predicted solar neutrino fluxes?*, *Astrophys. J.* **626** (2005) 530 [astro-ph/0412096] [inSPIRE].

[35] G. Battistoni, A. Ferrari, T. Montaruli and P.R. Sala, *The atmospheric neutrino flux below 100 MeV: the FLUKA results*, *Astropart. Phys.* **23** (2005) 526 [inSPIRE].

[36] I. Esteban, M.C. Gonzalez-Garcia, M. Maltoni, I. Martinez-Soler and J. Salvado, *Updated constraints on non-standard interactions from global analysis of oscillation data*, *JHEP* **08** (2018) 180 [arXiv:1805.04530] [inSPIRE].

[37] W. Rodejohann, X.-J. Xu and C.E. Yaguna, *Distinguishing between Dirac and Majorana neutrinos in the presence of general interactions*, *JHEP* **05** (2017) 024 [arXiv:1702.05721] [inSPIRE].

[38] Y. Farzan, M. Lindner, W. Rodejohann and X.-J. Xu, *Probing neutrino coupling to a light scalar with coherent neutrino scattering*, *JHEP* **05** (2018) 066 [arXiv:1802.05171] [inSPIRE].